- Macrocyclic depolymerization of arylene-ethynylene copolymers: a dynamic combinatorial method
  Gross, D. E.; Discekici, E.; Moore, J. S. *Chem. Commun.* **2012**, *48*, 4426-4428.
  Abstract:

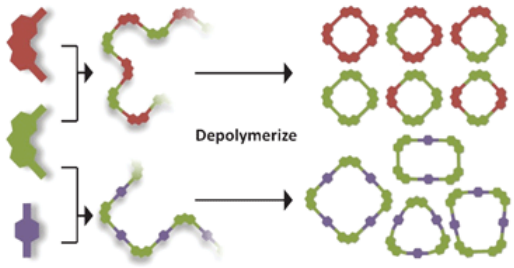

We report the synthesis of hybrid arylene-ethynylene macrocycles by alkyne metathesis enabled depolymerization.

- Twists and turns in the hierarchical self-assembly pathways of a non-amphiphilic chiral supramolecular material
  Danila, I.; Pop, F. ; Escudero, C.; Feldborg, L. N.; Luis, J. P.; Riobé, F.; Avarvari, N.; Amabilino, D. B. *Chem. Commun.* **2012**, *48*, 4552-4554.
  Abstract:

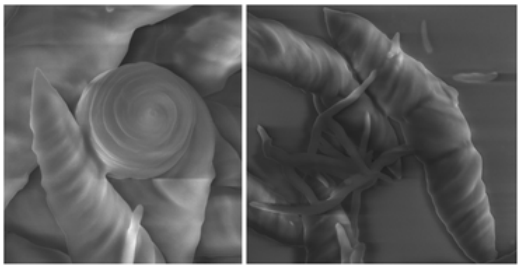

A variety of different chiral forms, including unprecedented croissants, are self-assembled from helical supramolecular fibres by varying the processing conditions.

- Novel self-assembled dynamic [2]catenanes interlocked by the quadruple hydrogen bonding ureidopyrimidinone motif
  Xiao, T.; Li, S. L.; Zhang, Y.; Lin, C.; Hu, B.; Guan, X.; Yu, Y.; Jiang, J.; Wang, L. *Chem. Sci.* **2012**, *3*, 1417-1421.
  Abstract:

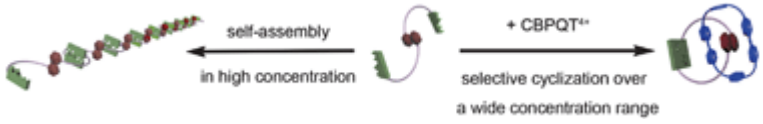

Novel dynamic donor–acceptor [2]catenanes interlocked by the quadruple hydrogen bonding ureidopyrimidinone motif have been constructed.

- Self-organizing surface-initiated polymerization of perylenediimides on indium tin oxides
  Charbonnaz, P.; Sakai, N.; Matile, S. *Chem. Sci.* **2012**, *3*, 1492-1496.
  Abstract:

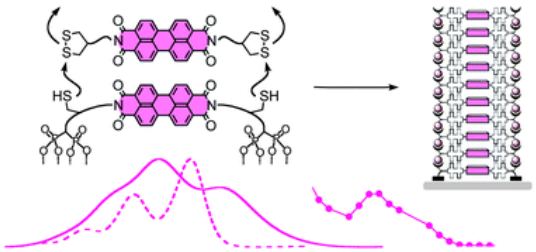

Perylenediimides (PDIs) are placed in photosystems made by SOSIP, a new, user-friendly route to oriented multicomponent architectures on solid surfaces.

- Direct Heteroarylation of Tautomerizable Heterocycles into Unsymmetrical and Symmetrical Biheterocycles via Pd/Cu-Catalyzed Phosphonium Coupling
  Sharma, A.; Vachhani, D.; Van der Eycken, E. *Org. Lett.* **2012**, *14*, 1854-1857.
  Abstract:

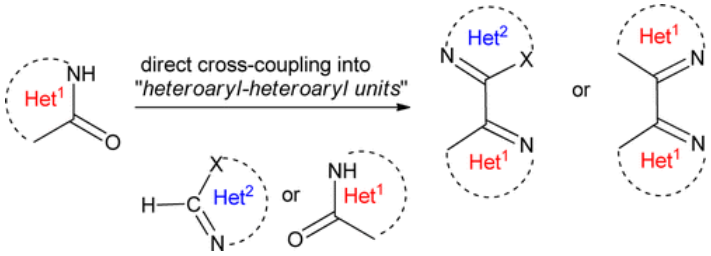

The direct cross-coupling of tautomerizable heterocycles with various unfunctionalized heteroarenes has been achieved through PyBroP-mediated and Pd/Cu-catalyzed sequential C–OH/C–H activation. The methodology allows a facile entry into novel diazine-azole biheterocyclic frameworks. Moreover, an unprecedented Pd-catalyzed phosphonium homocoupling of tautomerizable heterocycles was also developed to afford a direct synthetic route to symmetrical 1,2-, 1,3-, and 1,4-bidiazine units.

- 4-Methoxybenzyloxymethyl Group, a Racemization-Resistant Protecting Group for Cysteine in Fmoc Solid Phase Peptide Synthesis
  Hibino, H.; Nishiuchi, Y. *Org. Lett.* **2012**, *14*, 1926-1929.
  Abstract:

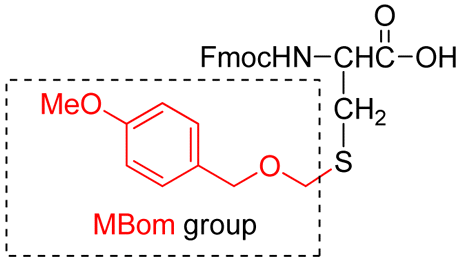

The 4-methoxybenzyloxymethyl (MBom) group was introduced for sulfhydryl protection of Cys in combination with Fmoc chemistry. The MBom group proved to substantially suppress racemization of Cys during its incorporation mediated by phosphonium or uronium reagents. Furthermore, this group was found to significantly reduce racemization of the C-terminal Cys linked to a hydroxyl resin during repetitive base treatment, in comparison with the usually used trityl (Trt) and acetamidomethyl (Acm) groups.

- New Organic Dye Based on a 3,6-Disubstituted Carbazole Donor for Efficient Dye-Sensitized Solar Cells

Lee, W.; Cho, N.; Kwon, J.; Ko, J.; Hong, J.-I. *Chem. Asian J.* **2012**, *7*, 343–350.

Abstract:

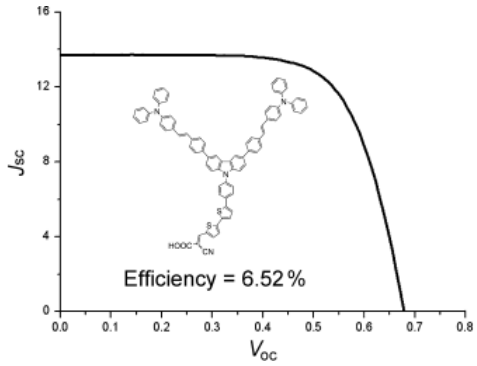

We have synthesized and characterized four organic dyes (**H1–H4**) based on a 3,6-disubstituted carbazole donor as sensitizers in dye-sensitized solar cells. These dyes have high molar extinction coefficients and energy levels suitable for electron transfer from an electrolyte to nanocrystalline TiO_2 particles. Under standard air mass 1.5 global (AM 1.5 G) solar irradiation, a device using dye **H4** exhibits a short-circuit current density (J_{sc}) of 13.7 mA cm^{-2}, an open-circuit voltage (V_{oc}) of 0.68 V, a fill factor (*FF*) of 0.70, and a calculated efficiency of 6.52 %. This performance is comparable to that of a reference cell based on N719 (7.30 %) under the same conditions. After 1000 hours of visible-light soaking at 60 °C, the overall efficiency remained at 95 % of the initial value.

- Synthesis and Spectroscopic Properties of Phthalocyanine–[60]Fullerene Conjugates Connected Directly by Means of a Four-Membered Ring

  Fukuda, T.; Kikukawa, Y.; Takaishi, S.; Kobayashi, N. *Chem. Asian J.* **2012**, *7*, 751–758.

  Abstract:

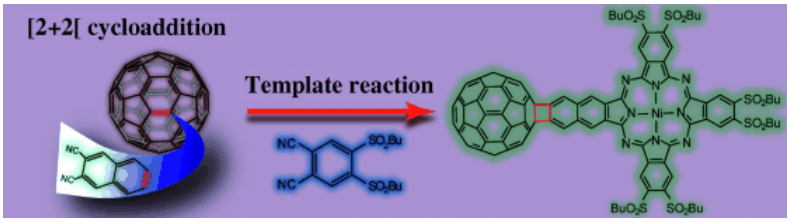

New covalently C_{60}-conjugated phthalocyanine (Pc) analogues in which the Pc and C_{60} components are connected by means of a four-membered ring have been synthesized by taking advantage of a [2+2] cycloaddition reaction of C_{60} with benzyne units generated from either a phthalocyanine derivative (**8**) or its precursor (**1**). The reaction of **1** with $PhI(OAc)_2$ and trifluoromethanesulfonic acid (TfOH) followed by the [2+2] cycloaddition of C_{60} in the presence of tetra-*n*-butylammonium fluoride (TBAF) yielded the C_{60}-substituted Pc precursor (**3**). Mixed condensation of **3** and 4,5-dibutylsulfonylphthalonitrile (**4**) in a thermally promoted template reaction using a nickel salt successfully gave the Pc–C_{60} conjugate (**5**). Results of mass spectrometry and ^{1}H and ^{13}C NMR spectroscopy clearly indicate the formation of the anticipated Pc–C_{60} conjugate. Direct coupling of C_{60} with the Pc analogue that contained eight peripheral trimethylsilyl (TMS) groups (**8**) also proceeded successfully, such that mono and bis C_{60}-adducts were detected by their mass, although the isolation of each derivative was difficult. The absorption and magnetic circular dichroism (MCD) spectra of **5** and the reference compound (**7**) differ from each other in the Q-band region, thereby suggesting that the presence of the C_{60} moiety affects the electronic structure of the conjugate. The reduction and oxidation potentials of **5** and **7** obtained by cyclic voltammetry are comparative, except for the C_{60}-centered reduction couple at −1.53 V versus Fc^+/Fc in *o*-dichlorobenzene (*o*-DCB). A one-electron

reduction of **5** and **7** in tetrahydrofuran (THF) by using the sodium mirror technique results in the loss of band intensity in the Q-band region, whereas the characteristic marker bands for Pc-ring-centered reduction appear at around 430, 600, and 900 nm for both compounds. The final spectral shapes of **5** and **7** upon the reduction resemble each other, thus indicating that no significant molecular orbital (MO) interactions between the C_{60} and Pc units are present for the reduced species of **5**. In contrast, the oxidized species of **5** and **7** generated by the addition of $NOBF_4$ in CH_2Cl_2 show significantly different absorption spectra from each other. Whereas the broad bands at approximately 400–550 nm of $\mathbf{7}^+$ are indicative of the cationic π-radical species of metallo-Pcs and can be assigned to a transition from a low-lying MO to the half-filled MO, no corresponding bands were observed for $\mathbf{5}^+$. These spectral characteristics have been tentatively assigned to the delocalized occupied frontier MOs for $\mathbf{5}^+$. The experimental results are broadly supported by DFT calculations.

- Minimalist Probes for Studying Protein Dynamics: Thioamide Quenching of Selectively Excitable Fluorescent Amino Acids
  Goldberg, J. M.; Speight, L. C.; Fegley, M. W.; Petersson, E. J. *J. Am. Chem. Soc.* **2012**, *134*, 6088–6091.
  Abstract:

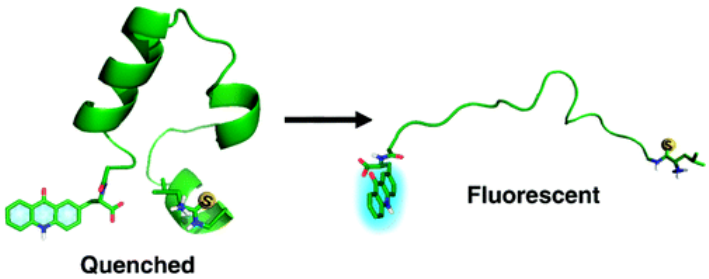

Fluorescent probe pairs that can be selectively excited in the presence of Trp and Tyr are of great utility in studying conformational changes in proteins. However, the size of these probe pairs can restrict their incorporation to small portions of a protein sequence where their effects on secondary and tertiary structure can be tolerated. Our findings show that a thioamide bond—a single atom substitution of the peptide backbone—can quench fluorophores that are red-shifted from intrinsic protein fluorescence, such as acridone. Using steady-state and fluorescence lifetime measurements, we further demonstrate that this quenching occurs through a dynamic electron-transfer mechanism. In a proof-of-principle experiment, we apply this technique to monitor unfolding in a model peptide system, the villin headpiece HP35 fragment. Thioamide analogues of the natural amino acids can be placed in a variety of locations in a protein sequence, allowing one to make a large number of measurements to model protein folding.

- Coordination and Metalation Bifunctionality of Cu with 5,10,15,20-Tetra(4-pyridyl)porphyrin: Toward a Mixed-Valence Two-Dimensional Coordination Network
  Li, Y.; Xiao, J.; Shubina, T. E.; Chen, M.; Shi, Z.; Schmid, M.; Steinrück, H.-P.; Gottfried, J. M.; Lin, N. *J. Am. Chem. Soc.* **2012**, *134*, 6401–6408.
  Abstract:

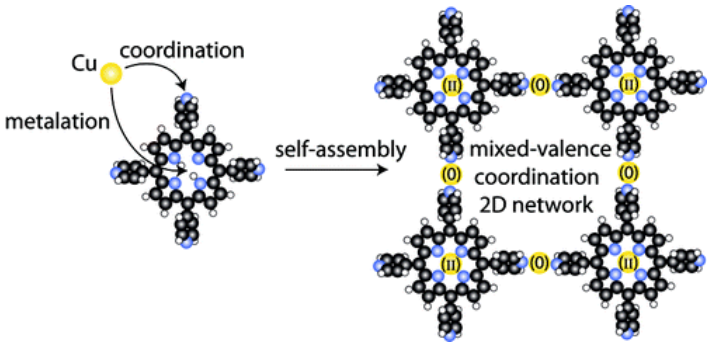

We investigated the coordination self-assembly and metalation reaction of Cu with 5,10,15,20-tetra(4-pyridyl)porphyrin (2HTPyP) on a Au(111) surface by means of scanning tunneling microscopy, X-ray photoelectron spectroscopy, and density functional theory calculations. 2HTPyP was found to interact with Cu through both the peripheral pyridyl groups and the porphyrin core. Pairs of pyridyl groups from neighboring molecules coordinate Cu(0) atoms, which leads to the formation of a supramolecular metal–organic coordination network. The network formation occurs at room temperature; annealing at 450 K enhances the process. The interaction of Cu with the porphyrin core is more complex. At room temperature, formation of an initial complex Cu(0)–2HTPyP is observed. Annealing at 450 K activates an intramolecular redox reaction, by which the coordinated Cu(0) is oxidized to Cu(II) and the complex Cu(II)TPyP is formed. The coordination network consists then of Cu(II) complexes linked by Cu(0) atoms; that is, it represents a mixed-valence two-dimensional coordination network consisting of an ordered array of Cu(II) and Cu(0) centers. Above 520 K, the network degrades and the Cu atoms in the linking positions diffuse into the substrate, while the Cu(II)TPyP complexes form a close-packed structure that is stabilized by weak intermolecular interactions. Density functional theory investigations show that the reaction with Cu(0) proceeds via formation of an initial complex between metal atom and porphyrin followed by formation of Cu(II) porphyrin within the course of the reaction. The activation barrier of the rate limiting step was found to be 24–37 kcal mol^{-1} depending on the method used. In addition, linear coordination of a Cu atom by two CuTPyP molecules is favorable according to gas-phase calculations.

- The Crowded Environment of a Reverse Micelle Induces the Formation of β-Strand Seed Structures for Nucleating Amyloid Fibril Formation
  Yeung, P. S. W.; Axelsen, P. H. *J. Am. Chem. Soc.* **2012**, *134*, 6061–6063.
  Abstract:

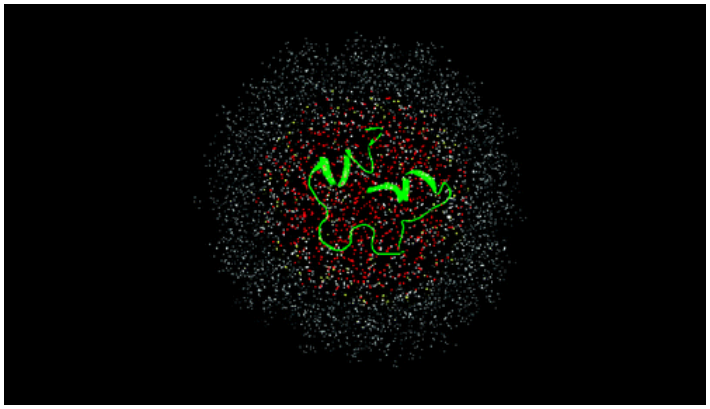

A hallmark of Alzheimer's disease is the accumulation of insoluble fibrils in the brain composed of amyloid beta (Aβ) proteins with parallel in-register cross-β-sheet structure. It has been suggested that the aggregation of monomeric Aβ proteins into fibrils is promoted by "seeds" that form within

compartments of the brain that have limited solvent due to macromolecular crowding. To characterize these seeds, a crowded macromolecular environment was mimicked by encapsulating Aβ40 monomers into reverse micelles. Fourier-transform infrared spectroscopy revealed that monomeric Aβ proteins form extended β-strands in reverse micelles, while an analogue with a scrambled sequence does not. This is a remarkable finding, because the formation of extended β-strands by monomeric Aβ proteins suggests a plausible mechanism whereby the formation of amyloid fibrils may be nucleated in the human brain.

- Interpreting Protein Structural Dynamics from NMR Chemical Shifts
  Robustelli, P.; Stafford, K. A.; Palmer, III, A. G. *J. Am. Chem. Soc.* **2012**, *134*, 6365–6374.
  Abstract:

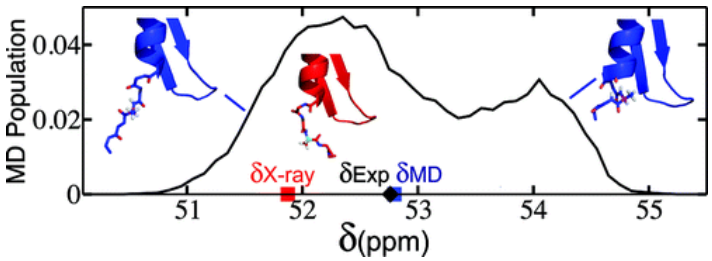

In this investigation, semiempirical NMR chemical shift prediction methods are used to evaluate the dynamically averaged values of backbone chemical shifts obtained from unbiased molecular dynamics (MD) simulations of proteins. MD-averaged chemical shift predictions generally improve agreement with experimental values when compared to predictions made from static X-ray structures. Improved chemical shift predictions result from population-weighted sampling of multiple conformational states and from sampling smaller fluctuations within conformational basins. Improved chemical shift predictions also result from discrete changes to conformations observed in X-ray structures, which may result from crystal contacts, and are not always reflective of conformational dynamics in solution. Chemical shifts are sensitive reporters of fluctuations in backbone and side chain torsional angles, and averaged ^{1}H chemical shifts are particularly sensitive reporters of fluctuations in aromatic ring positions and geometries of hydrogen bonds. In addition, poor predictions of MD-averaged chemical shifts can identify spurious conformations and motions observed in MD simulations that may result from force field deficiencies or insufficient sampling and can also suggest subsets of conformational space that are more consistent with experimental data. These results suggest that the analysis of dynamically averaged NMR chemical shifts from MD simulations can serve as a powerful approach for characterizing protein motions in atomistic detail.

- Correlating Structure with Function in Thermally Annealed PCDTBT:PC70BM Photovoltaic Blends
  Wang, T.; Pearson, A. J.; Dunbar, A. D. F.; Staniec, P. A.; Watters, D. C.; Yi, H.; Ryan, A. J.; Jones, R. A. L.; Iraqi, A.; Lidzey, D. G. *Adv. Funct. Mater.* **2012**, *22*, 1399–1408.
  Abstract:

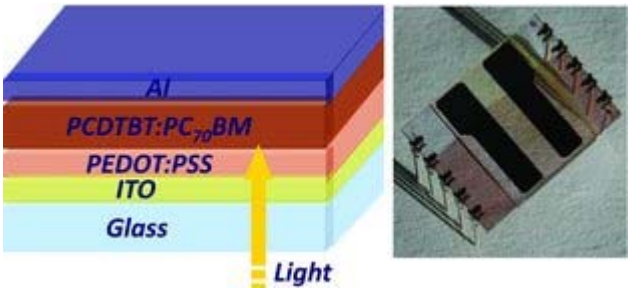

A range of optical probes are used to study the nanoscale-structure and electronic-functionality of a photovoltaic-applicable blend of the carbazole co-polymer poly[*N*-9′-heptadecanyl-2,7-carbazole-alt-5,5-(4′,7′-di-2-thienyl-2′,1′,3′-benzothiadiazole) (PCDTBT) and the electronic accepting fullerene derivative (6,6)-phenyl C_{70}-butyric acid methyl ester ($PC_{70}BM$). In particular, it is shown that the glass transition temperature of a PCDTBT:$PC_{70}BM$ blend thin-film is not sensitive to the relative blend-ratio or film thickness (at 1:4 blending ratio), but is sensitive to casting solvent and the type of substrate on which it is deposited. It is found that the glass transition temperature of the blend reduces on annealing; an observation consistent with disruption of π–π stacking between PCDTBT molecules. Reduced π–π stacking is correlated with reduced hole-mobility in thermally annealed films. It is suggested that this explains the failure of such annealing protocols to substantially improve device-efficiency. The annealing studies demonstrate that the blend only undergoes coarse phase-separation when annealed at or above 155 °C, suggesting a promising degree of morphological stability of PCDTBT:$PC_{70}BM$ blends.

- The Effect of Ageing on Exciton Dynamics, Charge Separation, and Recombination in P3HT/PCBM Photovoltaic Blends
  Deschler, F.; De Sio, A.; von Hauff, E.; Kutka, P.; Sauermann, T.; Egelhaaf, H.-J.; Hauch, J.; Da Como, E. *Adv. Funct. Mater.* **2012**, *22*, 1461–1469.
  Abstract:

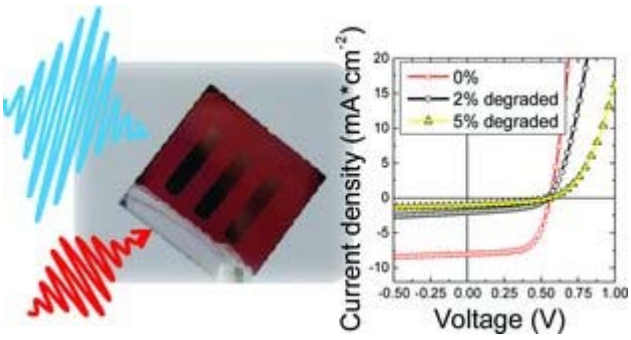

A study of how light-induced degradation influences the fundamental photophysical processes in the active layer of poly(3-hexylthiophene)/[6,6]-phenyl C_{61}-butyric acid methyl ester (P3HT/PCBM) solar cells is presented. Non-encapsulated samples are systematically aged by exposure to AM 1.5 illumination in the presence of dry air for different periods of time. The extent of degradation is quantified by the relative loss in the absorption maximum of the P3HT, which is varied in the range 0% to 20%. For degraded samples an increasing loss in the number of excitons within the P3HT domains is observed with longer ageing periods. This loss occurs rapidly, within the first 15 ps after photoexcitation. A more pronounced decrease in the population of polarons than excitons is observed, which also occurs on a timescale of a few picoseconds. These observations, complemented by a quantitative analysis of the polaron and exciton population dynamics, unravel two primary loss mechanisms for the performances of aged P3HT/PCBM solar cells. One is an initial ultrafast decrease

in the polaron generation, apparently not related to the exciton diffusion to the polymer/fullerene interface; the second, less significant, is a loss in the exciton population within the photoexcited P3HT domains. The steady-state photoinduced absorption spectra of degraded samples exhibits the appearance of a signal ascribed to triplet excitons, which is absent for non-degraded samples. This latter observation is interpreted considering the formation of degraded sites where intersystem crossing and triplet exciton formation is more effective. The photovoltaic characteristics of same blends are also studied and discussed by comparing the decrease in the overall power conversion efficiency of solar cells.

- Biaxially Extended Quaterthiophene– and Octithiophene–Vinylene Conjugated Polymers for High Performance Field Effect Transistors and Photovoltaic Cells
  Lu, C.; Wu, H. C.; Chiu, Y. C.; Lee, W. Y.; Chen, W. C. *Macromolecules* **2012**, *45*, 3047–3056.
  Abstract:

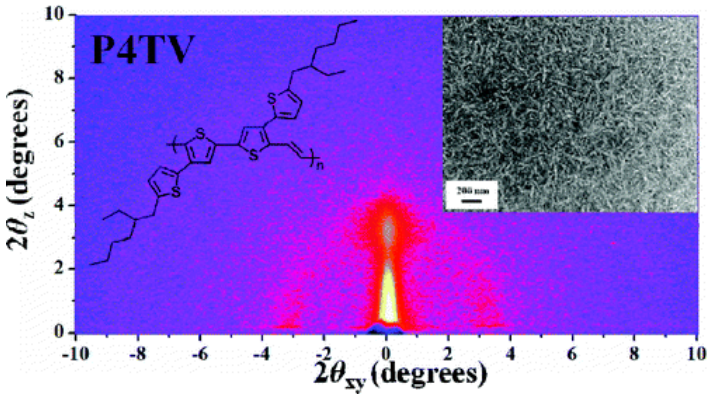

We report the synthesis, morphology, and optoelectronic device applications of novel biaxially extended quaterthiophene– (**4T**–) and octithiophene– (**8T**–) vinylene conjugated polymers, **P4TV** and **P8TV**, synthesized via Stille coupling reactions. **P4TV** and **P8TV** exhibited smaller energy band gaps of 1.69 and 1.78 eV than that of parent polythiophenes, respectively, due to the reduced conformation distortion by the vinylene linkage. The HOMO energy levels of **P4TV** and **P8TV** were −5.02 and −5.13 eV, respectively, resulting in air stable device performance. The highest field effect hole mobilities of **P4TV** and **P8TV** were 0.12 and 0.0018 $cm^2\ V^{-1}\ s^{-1}$, respectively, with on/off ratios around 10^4–10^5. The higher carrier mobility of **P4TV** was related to its ordered structure as evidenced from the TEM, AFM, and grazing incidence X-ray diffraction results. The power conversion efficiency (PCE) of the **P4TV/** $PC_{71}BM$ based photovoltaic cells (PV) under the illumination of AM 1.5G (100 mW/cm^2) was 4.04%, which was significantly higher than that of **P8TV**/$PC_{71}BM$ with 2.69%, due to its superior charge transport ability. However, **P8TV** had a better environmental stability attributed to its low-lying HOMO energy level. These above results demonstrate that biaxially extended thiophene–vinylene conjugated copolymers could be promising materials for high performance organic electronic device applications.

- *n*-Type Semiconducting Polymer Fibers
  Canesi, E. V.; Luzio, A.; Saglio, B.; Bianco, A.; Caironi, M.; Bertarelli, C. *ACS Macro Lett.*, **2012**, *1*, 366–369.
  Abstract:

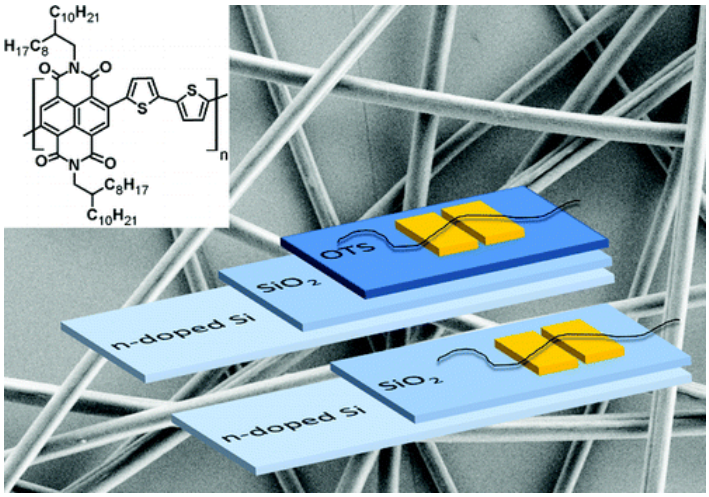

Defect-free bicomponent fibers of poly{[*N*,*N*′-bis(2-octyl-dodecyl)-naphthalene-1,4,5,8-bis(dicarboximide)-2,6-diyl]-*alt*-5,5′-(2,2′-bithiophene)}/poly(ethyleneoxide) P(NDI2OD-T2)/PEO are fabricated by means of electrospinning and rinsed with a selective solvent to afford pure P(NDI2OD-T2) while maintaining a fibrous morphology. The elongation strength applied on the spun jet by the high electrical field induces a preferential orientation of polymer chains. An electron mobility analogous to the best obtained with a thin film-based device is achieved in single fiber transistors, and the results are unaffected by the dielectric surface treatment.

- Reversible ON/OFF Nanoswitch for Organocatalysis: Mimicking the Locking and Unlocking Operation of CaMKII
  Schmittel, M., De, S.; Pramanik, S. *Angew. Chem. Int. Ed.* **2012**, *51*, 3832-3836.
  Abstract:

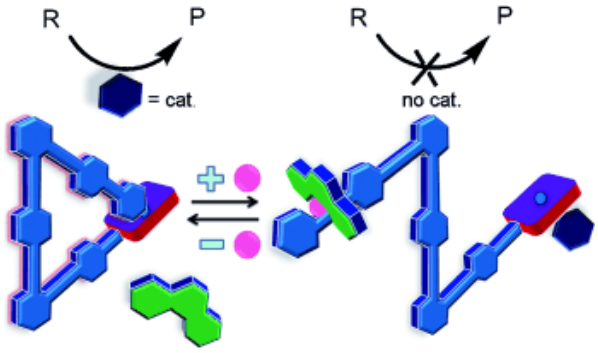

Flip a switch: A nanoswitch uses chemical inputs to turn an organocatalytic Knoevenagel reaction on and off (see scheme: R=reactant, P=product). To stop catalysis the chemical input (pink and green) wraps around the inhibitory segment of the nanoswitch to effect release or unlocking of the switch. The process can run reversibly over three cycles without loss of activity.

- Caged Glutathione – Triggering Protein Interaction by Light
  Farrington, B. J.; Jevric, M.; Gatterdam, V.; Stoess, T.; Menge, C.; Heckel, A.; Tampé, R. *Angew. Chem. Int. Ed.* **2012**, *51*, 3960-3963.
  Abstract:

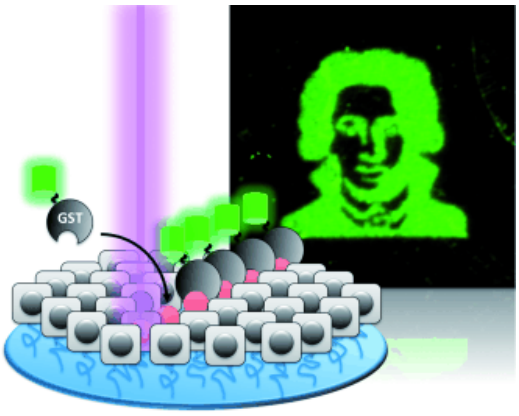

Light, GSH, action! Glutathione (GSH) fulfills a universal role as redox factor, scavenger of reactive oxygen species, and as an essential substrate in the conjugation, detoxification, and reduction reactions catalyzed by glutathione S-transferase (GST). A photoactivatable glutathione allows the GSH-GST network to be triggered by light. GST fusion proteins can be assembled in situ at variable density and structures by laser-scanning activation.

- High-valent organometallic copper and palladium in catalysis
  Hickman, A. J.; Sanford, M. S. *Nature* **2012**, *484*,177-185.
  Abstract:

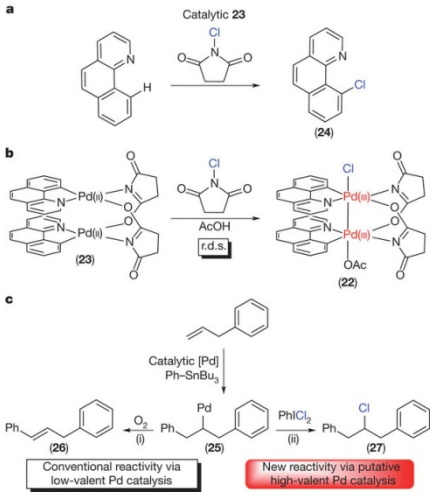

Copper and palladium catalysts are critically important in numerous commercial chemical processes. Improvements in the activity, selectivity and scope of these catalysts could drastically reduce the environmental impact, and increase the sustainability, of chemical reactions. One rapidly developing strategy for achieving these goals is to use 'high-valent' organometallic copper and palladium intermediates in catalysis. Here we describe recent advances involving both the fundamental chemistry and the applications of these high-valent metal complexes in numerous synthetically useful catalytic transformations.

- Edge-carboxylated graphene nanosheets via ball milling
  Jeon, I.-Y.; Shin, Y.-R.; Sohn, G.-J.; Choi, H.-J.; Bae, S.-Y.; Mahmood, J.; Jung, S.-M.; Seo, J.-M.; Kima, M.-J.; Chang, D. W.; Dai, L.; Baek, J. B. *Proc. Nat. Acad. Sci. USA* **2012**, *109*, 5588-5593.
  Abstract:

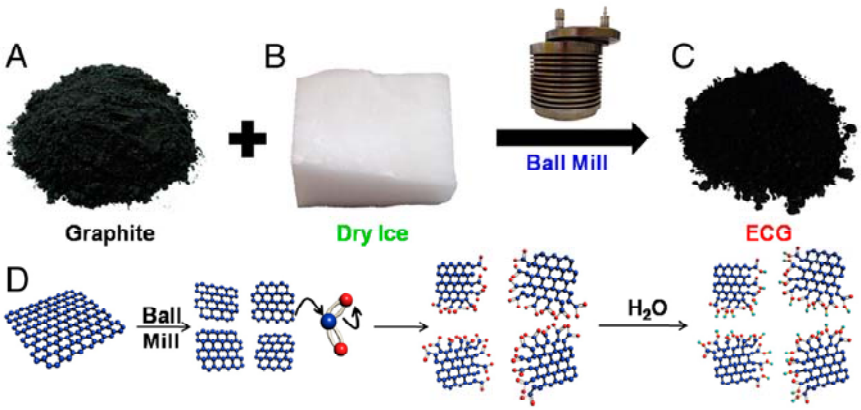

Low-cost, high-yield production of graphene nanosheets (GNs) is essential for practical applications. We have achieved high yield of edge-selectively carboxylated graphite (ECG) by a simple ball milling of pristine graphite in the presence of dry ice. The resultant ECG is highly dispersable in various solvents to self-exfoliate into single and few-layer (≤5 layers) GNs. These stable ECG (or GN) dispersions have been used for solution processing, coupled with thermal decarboxylation, to produce large-area GN films for many potential applications ranging from electronic materials to chemical catalysts. The electrical conductivity of a thermally decarboxylated ECG film was found to be as high as 1214 S/cm, which is superior to its GO counterparts. Ball milling can thus provide simple, but efficient and versatile, and eco-friendly (CO_2 -capturing) approaches to low-cost mass production of high-quality GNs for applications where GOs have been exploited and beyond.

- Ferroelectric Columnar Liquid Crystal Featuring Confined Polar Groups Within Core-Shell Architecture
  Miyajima, D.; Araoka, F.; Takezoe, H.; Kim, J.; Kato, K.; Takata, M.; Aida, T. *Science* **2012***, 336*, 209-213.
  Abstract:

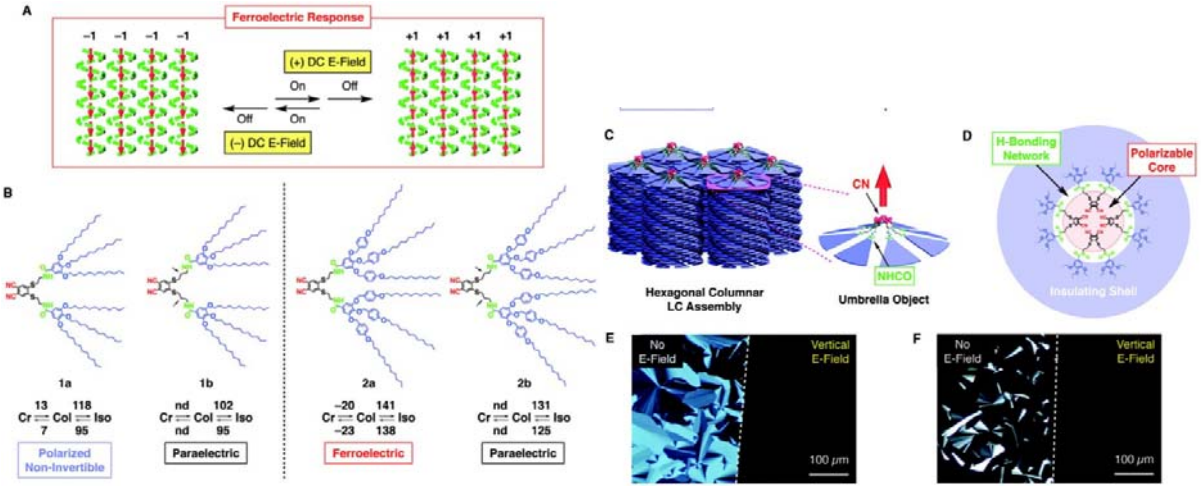

Ferroelectric liquid crystals are materials that have a remnant and electrically invertible polar order. Columnar liquid crystals with a ferroelectric nature have potential use in ultrahigh-density memory devices, if electrical polarization occurs along the columnar axis. However, columnar liquid crystals having an axial nonzero polarization at zero electric field and its electrical invertibility have not been demonstrated. Here, we report a ferroelectric response for a columnar liquid crystal adopting a core-shell architecture that accommodates an array of polar cyano groups confined by a hydrogen-bonded amide network with an optimal strength. Under an applied electric field, both columns and core

cyano groups align unidirectionally, thereby developing an extremely large macroscopic remnant polarization.

- Recent advances in solar cells based on one-dimensional nanostructure arrays
  Yu, M.; Long, Y.-Z.; Sun, B.; Fan, Z. *Nanoscale* **2012**, *4*, 2783-2796.
  Abstract:

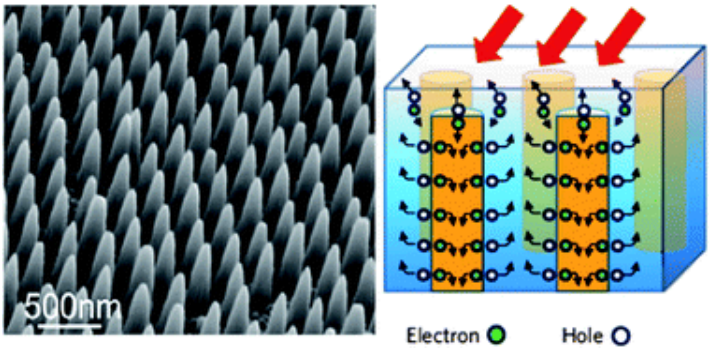

As the demand for renewable energy resource is growing rapidly worldwide, a variety of energy materials and technologies are being developed. In this review, we aim to summarize recent developments in the state-of-the-art research on energy harvesting technologies such as thin-film Si or Ge, CdTe, GaAs, organic, hybrid, and dye-sensitized solar cells (DSSCs) utilizing one-dimensional (1D) nanomaterials, mainly semiconductor nanowires, nanocones, nanotubes and nanofibers, which are prepared by vapor–liquid–solid method, colloidal lithography, template-guided growth, or electrospinning. Moreover, the future challenges (such as efficiency improvement and natural resource limitations) and prospects of nanostructured solar cells are proposed.

- Nanotube-Bridged Wires with Sub-10 nm Gaps
  Lee, B. Y.; Heo, K.; Schmucker, A. L.; Jin, H. J.; Lim, J. K.; Kim, T.; Lee, H.; Jeon, K.-S.; Suh, Y. D.; Mirkin, C. A.; Hong, S. *Nano Letters* **2012**, *12*, 1879-1884.
  Abstract:

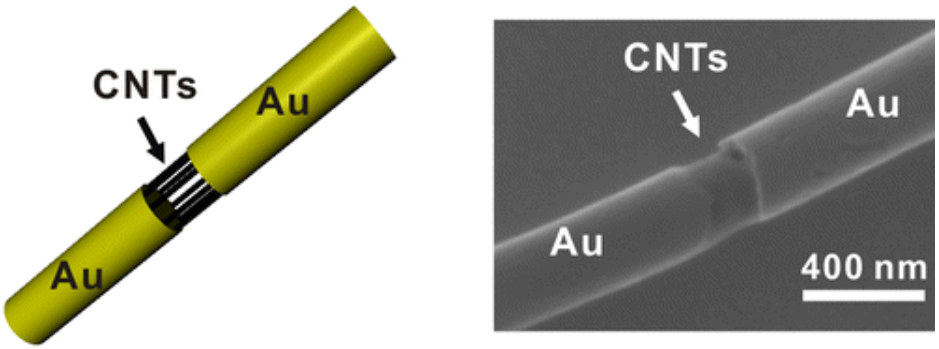

We report a simple but efficient method to synthesize carbon nanotube-bridged wires (NBWs) with gaps as small as 5 nm. In this method, we have combined a strategy for assembling carbon nanotubes (CNTs) inside anodized aluminum oxide pores and the on-wire lithography technique to fabricate CNT-bridged wires with gap sizes deliberately tailored over the 5–600 nm range. As a proof-of-concept demonstration of the utility of this architecture, we have prepared NBW-based chemical and biosensors which exhibit higher analyte sensitivity (lower limits of detection) than those based on planar CNT networks. This observation is attributed to a greater surface-to-volume ratio of CNTs in the NBWs than those in the planar CNT devices. Because of the ease of synthesis and high yield of

NBWs, this technique may enable the further incorporation of CNT-based architectures into various nanoelectronic and sensor platforms.

- Delivery of Small Interfering RNA by Peptide-Targeted Mesoporous Silica Nanoparticle-Supported Lipid Bilayers
  Ashley, C. E.; Carnes, E. C.; Epler, K. E.; Padilla, D. P.; Phillips, G. K.; Castillo, R. E.; Wilkinson, D. C.; Wilkinson, B. S.; Burgard, C. A.; Kalinich, R. M.; Townson, J. L.; Chackerian, B.; Willman, C. L.; Peabody, D. S.; Wharton, W.; Brinker, C. J. *ACS Nano* **2012**, *6*, 2174-2188.
  Abstract:

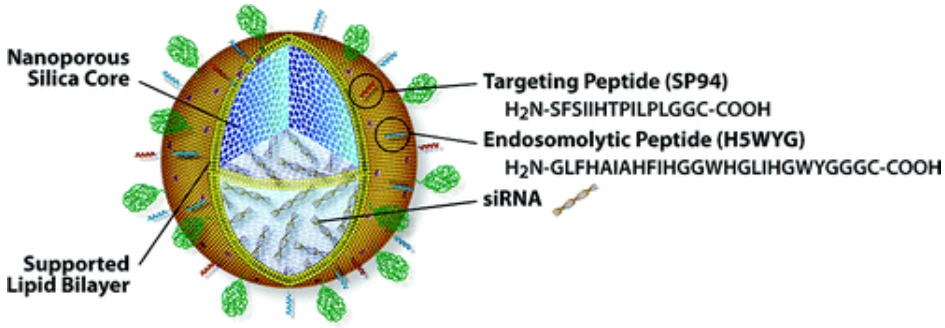

The therapeutic potential of small interfering RNAs (siRNAs) is severely limited by the availability of delivery platforms that protect siRNA from degradation, deliver it to the target cell with high specificity and efficiency, and promote its endosomal escape and cytosolic dispersion. Here we report that mesoporous silica nanoparticle-supported lipid bilayers (or “protocells”) exhibit multiple properties that overcome many of the limitations of existing delivery platforms. Protocells have a 10- to 100-fold greater capacity for siRNA than corresponding lipid nanoparticles and are markedly more stable when incubated under physiological conditions. Protocells loaded with a cocktail of siRNAs bind to cells in a manner dependent on the presence of an appropriate targeting peptide and, through an endocytic pathway followed by endosomal disruption, promote delivery of the silencing nucleotides to the cytoplasm. The expression of each of the genes targeted by the siRNAs was shown to be repressed at the protein level, resulting in a potent induction of growth arrest and apoptosis. Incubation of control cells that lack expression of the antigen recognized by the targeting peptide with siRNA-loaded protocells induced neither repression of protein expression nor apoptosis, indicating the precise specificity of cytotoxic activity. In terms of loading capacity, targeting capabilities, and potency of action, protocells provide unique attributes as a delivery platform for therapeutic oligonucleotides.

- Full Characterization of Colloidal Solutions of Long-Alkyl-Chain-Amine-Stabilized ZnO Nanoparticles by NMR Spectroscopy: Surface State, Equilibria, and Affinity
  Coppel, Y.; Spataro, G.; Pagès, C.; Chaudret, B.; Maisonnat, A.; Kahn, M. L. *Chem. Eur. J.* **2012**, *18*, 5384 – 5393.
  Abstract:

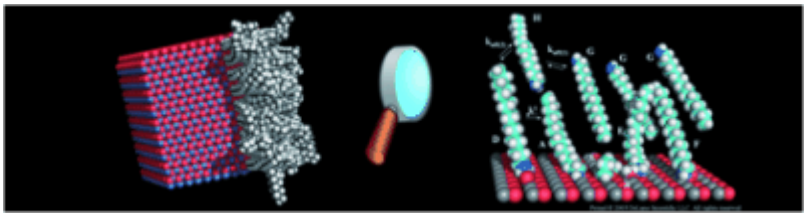

The long-chain home: The surface of ZnO nanoparticles stabilized by amines was fully characterized by NMR spectroscopy. The apparently simple stabilization of ZnO nanoparticles by amines turned out to be far more complex than thought.

- Design, Synthesis, and Miniemulsion Polymerization of New Phosphonate Surfmers and Application Studies of the Resulting Nanoparticles as Model Systems for Biomimetic Mineralization and Cellular Uptake
  Sauer, R.; Froimowicz, P.; Schöller, K.; Cramer, J. M.; Ritz, S.; Mailänder, V.; Landfester, K. *Chem. Eur. J.* **2012**, *18*, 5201 – 5212.
  Abstract:

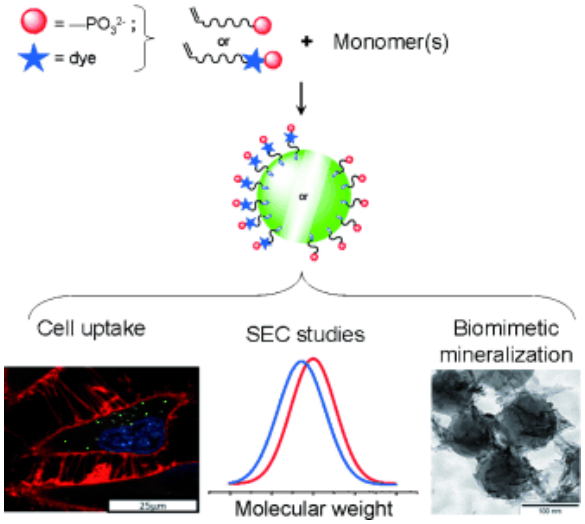

Functional surfmers: The specific design, synthesis, optimization, and application of a (dye-containing) surfmer family bearing phosphonic acid as the polar-head and methacrylamide as the polymerizable group enables the use of the subsequently synthesized latexes as model systems to study selective surface functionalization, surfmer copolymerization efficiency, and diverse ways to successfully exploit them in different fields such as biomimetic mineralization and cell uptake (see figure).

- Controlled Growth of Polyaniline Fractals on HOPG through Potentiodynamic Electropolymerization
  Bhattacharjya, D.; Mukhopadhyay, I. *Langmuir* **2012**, *28*, 5893–5899.
  Abstract:

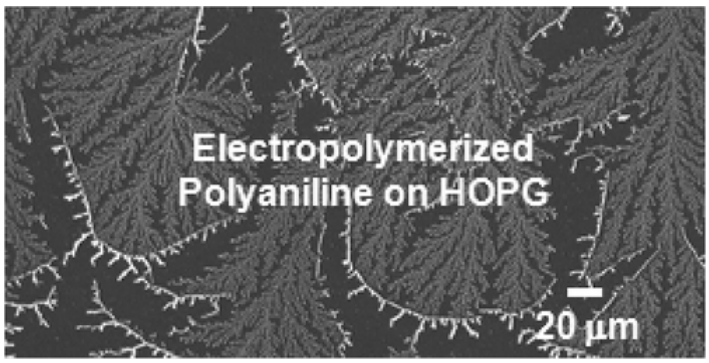

Polyaniline (PANI) in fractal dimension has been electrodeposited reproducibly on highly oriented pyrolytic graphite (HOPG) from 0.2 M aniline in 1 M aqueous HCl solution by potentiodynamic sweeping in the range of −0.2 to 0.76 V vs Ag/AgCl at room temperature. Fractal growth of PANI

dendrimers is affected by diffusion limited polymerization (DLP) at a sweep rate of 15 mV s^{-1} for 43 min. This type of PANI dendrimer is prepared for the first time on such large area HOPG substrate by electrochemical technique using rather simple cell setup. The fractal dimension has been determined by chronoamperometry (CA) and box counting technique and is found to vary from 1.4 to 1.9 with the duration of electropolymerization. The sweep rate, terminal oxidation potential, and the diverse surface anisotropy of the HOPG surface are found to be crucial factors in controlling the growth of such PANI fractals.

- Coordination Structures and Supramolecular Architectures in a Cerium(III)–Malonamide Solvent Extraction System
  Ellis, R. J.; Antonio, M. R. *Langmuir* **2012**, *28*, 5987–5998.
  Abstract:

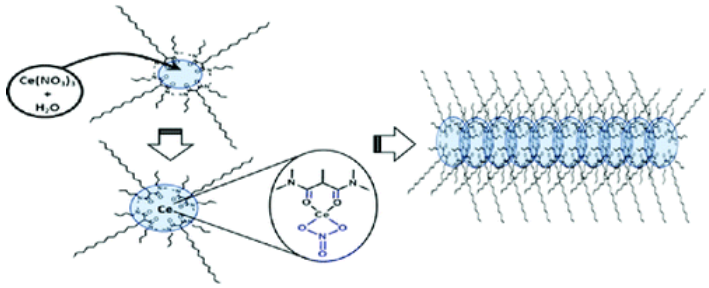

The process chemistry and solution structures investigated in the title system bridge the three ostensibly disparate fields of separation sciences, soft matter research, and coordination chemistry. We have explored this subject with synchrotron radiation research and advanced analyses leading to original insights into aggregation phenomena in solvent extraction. Herein we present findings showing the coagulation of reverse micelles into wormlike aggregates in organic phases (*N*,*N*′-dimethyl-*N*,*N*′-dibutyltetradecylmalonamide—abbreviated as DMDBTDMA—in *n*-dodecane) obtained by liquid–liquid extraction following contact with acidic and neutral aqueous media containing trivalent cerium. The growth of solute architectures was shown to prelude phase transition (i.e., the formation of a “third phase”). The presence of acid was shown to promote the growth of these micellar chains and, therefore, promoted third-phase formation. Acid was also shown to hydrate and swell the reverse micelle units, preorganizing them to allow for incorporation of cerium, leading to different coordination structures and enhanced metal extraction. The approach of linking both the coordination environment and supramolecular structures to the process properties of a solvent extraction system in a single study provides perspectives that are not available from independent, uncorrelated experimentation. Moreover, the analysis of small-angle X-ray scattering data from a solvent extraction system using the generalized indirect Fourier transform method to gain real-space information led to insights not otherwise available, showing that micellar assemblies are larger and more ordered than previously thought. This multipronged and multidisciplinary investigation opens new avenues in the evolving understanding of solute architectures in organic phases of practical relevance to solvent extraction and, simultaneously, of fundamental relevance to structured fluids and, in particular, phase transition phenomena.

- Autonomous movement of platinum-loaded stomatocytes
  Wilson, D. A.; Nolte, R. J. M.; Hest, J. C. M. *Nature Chemistry* **2012**, *4*, 268–274.
  Abstract:

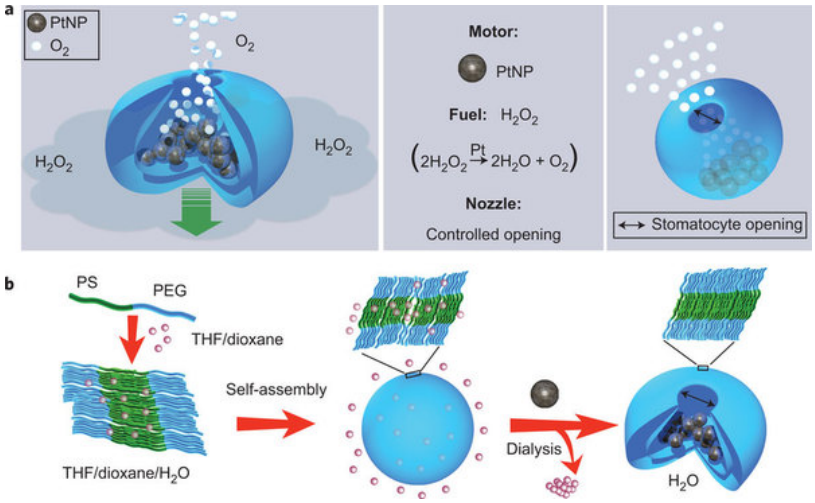

Polymer stomatocytes are bowl-shaped structures of nanosize dimensions formed by the controlled deformation of polymer vesicles. The stable nanocavity and strict control of the opening are ideal for the physical entrapment of nanoparticles which, when catalytically active, can turn the stomatocyte morphology into a nanoreactor. Herein we report an approach to generate autonomous movement of the polymer stomatocytes by selectively entrapping catalytically active platinum nanoparticles within their nanocavities and subsequently using catalysis as a driving force for movement. Hydrogen peroxide is free to access the inner stomatocyte cavity, where it is decomposed by the active catalyst (the entrapped platinum nanoparticles) into oxygen and water. This generates a rapid discharge, which induces thrust and directional movement. The design of the platinum-loaded stomatocytes resembles a miniature monopropellant rocket engine, in which the controlled opening of the stomatocytes directs the expulsion of the decomposition products away from the reaction chamber (inner stomatocyte cavity).

- Mesoporous organohydrogels from thermogelling photocrosslinkable nanoemulsions
  Helgeson, M. E.; Moran, S. E.; An, H. Z.; Doyle, P. S. *Nature Materials* **2012**, *11*, 344–352.
  Abstract:

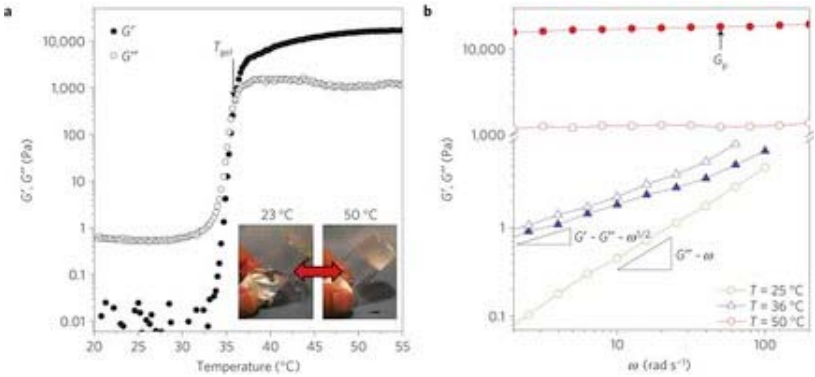

We report the formation of mesoporous organohydrogels from oil-in-water nanoemulsions containing an end-functionalized oligomeric gelator in the aqueous phase. The nanoemulsions exhibit an abrupt thermoreversible transition from a low-viscosity liquid to a fractal-like colloidal gel of droplets with mesoscale porosity and solid-like viscoelasticity with moduli approaching 100 kPa, possibly the highest reported for an emulsion-based system. We hypothesize that gelation is brought about by temperature-induced interdroplet bridging of the gelator, as shown by its dependence on the gelator chemistry. The use of photocrosslinkable gelators enables the freezing of the nanoemulsion's microstructure into a soft hydrogel nanocomposite containing a large fraction of

dispersed liquid hydrophobic compartments, and we show its use in the encapsulation and release of lipophilic biomolecules. The tunable structural, mechanical and optical properties of these organohydrogels make them a robust material platform suitable for a wide range of applications.

- Mechanisms of Nucleophilic Organocopper(I) Reactions
  Yoshikai, N.; Nakamura, E. *Chem. Rev.* **2012**, *112*, 2339-2372.
  Abstract:

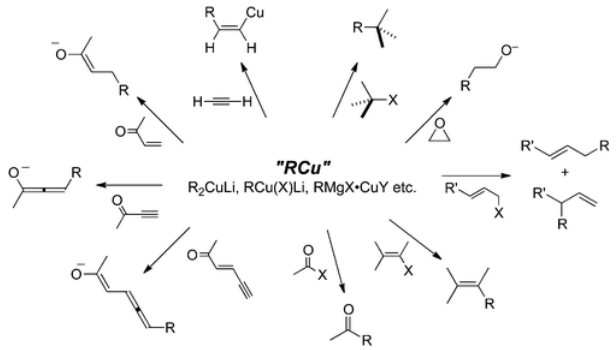

In this review, we will describe what we know in 2011 on the mechanism of the reactions of nucleophilic organocopper(I) reagents as viewed through a window of molecular orbital analysis supplemented by experimental data on structures in solution and in the solid state. A comprehensive mechanistic picture of representative organocopper(I)-mediated C–C bond-forming reactions in Scheme 1 will be illustrated. It should be noted that, while conventional organocopper reagents continue to be important synthetic tools, the expected depletion of rare metal elements has aroused new interest in the use of copper as a ubiquitous, base metal for organic synthesis and catalysis. In this regard, we hope that this review not only serves as a mechanistic overview of established organocopper reactions but also provides inspiration for designing new organocopper-mediated/catalyzed transformations.

- Attaching Persistent Organic Free Radicals to Surfaces: How and Why
  Mas-Torrent, M.; Crivillers, N.; Rovira, C.; Veciana, J. *Chem. Rev.* **2012**, *112*, 2506-2527.
  Abstract:

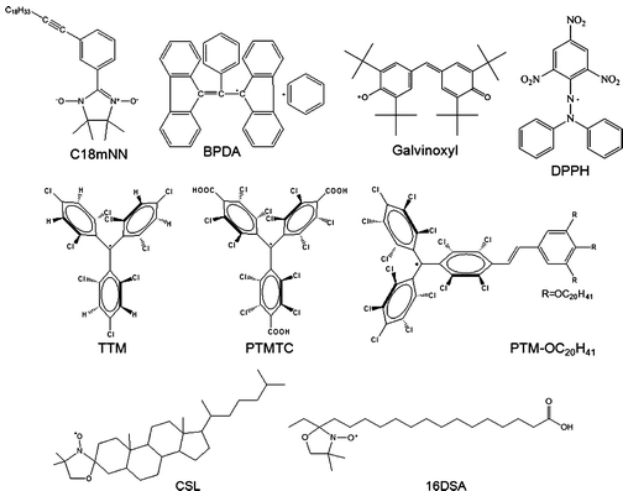

The scope of this review is to overview the recent progress devoted to the organization of monolayers of these magnetic molecules on surfaces, paying particular attention to the preparation, characterization, and future perspectives of this novel-type of materials.

- Quinacridone-Based Semiconducting Polymers: Implication of Electronic Structure and Orientational Order for Charge Transport Property
  Osaka, I.; Akita, M.; Koganezawa, T.; Takimiya, K. *Chem. Mater.* **2012**, *24*, 1235–1243.
  Abstract:

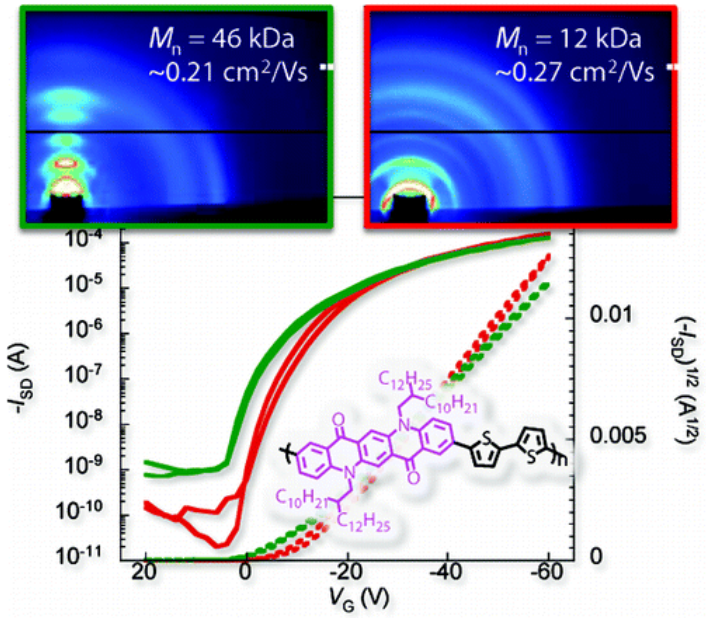

We report the synthesis, characterization, and field-effect transistor properties of novel semiconducting polymers, PQA2T and PQA3T, incorporating a quinacridone unit, and discuss the structure–property relationships. Comparison of the optical and electrochemical properties between the monomer, repeat unit, and polymer suggests that the effective π-conjugation and the delocalization of HOMO along the backbone are relatively limited. X-ray diffraction studies revealed that the polymers form a π–π stacking with a short distance of 3.6 Å and that the orientational order was enhanced by an increase of molecular weight. The hole mobilities are found to be around 0.2 $cm^2\ V^{-1}\ s^{-1}$ and are, interestingly, insensitive to the molecular weight and to the orientational order; the randomly oriented low molecular weight polymer showed similar mobilities to the edge-on oriented high molecular weight polymer. We speculate that the relatively localized HOMO might hinder the charge transport along the backbone, and thus the longer polymer chain is not necessary to facilitate the charge transport. The locally but strongly π–π interacted polymer crystallites seem to be sufficient for the effective charge transport in the QA-based polymer system. These features in the present polymers offer great interest of using QA moieties as the building block for semiconducting polymers and give new insight into the design of a new class of semiconducting polymers.

- Helically π-Stacked Thiophene-Based Copolymers with Circularly Polarized Fluorescence: High Dissymmetry Factors Enhanced by Self-Ordering in Chiral Nematic Liquid Crystal Phase
  Watanabe, K.; Osaka, I.; Yorozuya, S.; Akagi, K. *Chem. Mater.* **2012**, *24*, 1011–1024.
  Abstract:

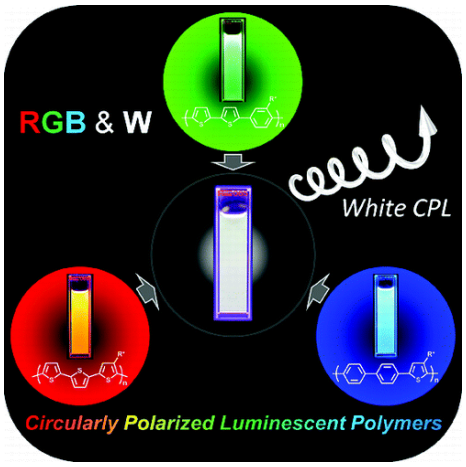

Novel derivatives of polythiophenes and their phenylene copolymers were synthesized by introducing chiral alkoxy carbonyl substituents into their side chains. Most of these polymers showed enantiotropic main-chain liquid crystallinity at high temperatures and across a wide range of elevated temperatures. They exhibited fluorescence that ranged in color from blue to orange in chloroform solutions and from blue to red in films. The bisignate Cotton effect was observed in the π–π* transition region of the circular dichroism (CD) spectra of the polymers consisting of three aromatic rings in the repeating unit, which was attributed to the formation of a polymer assembly with an interchain helically π-stacked structure. The dependence of UV–vis absorption and CD spectra on the concentration and temperature of the solution indicated that the polymer assembly exists, even in dilute concentration at room temperature, but it dissociated into single polymers at high temperatures. Additionally, the polymer films exhibited an enhanced Cotton effect caused by the strengthening of the helical π-stacking in the polymer assembly. Both the polymer solutions and films generated circularly polarized fluorescence with values for g_{em}, the dissymmetry factor, on the order of 10^{-3} and 10^{-2}, respectively. Values for g_{em} as high as 10^{-1} were obtained by annealing the polymer films at temperatures corresponding to the liquid crystalline region and were due to the self-ordering of their chiral nematic phases. Furthermore, a mixture of red, green, and blue fluorescent polymers generated a unique, circularly polarized white luminescence not only in solution but also in the cast film prepared by dispersing the mixture in an excess of polystyrene.